Exploring binding mode for styrylquinoline HIV-1 integrase inhibitors using comparative molecular field analysis and docking studies[1]

Xiao-hui MA, Xiao-yi ZHANG, Jian-jun TAN, Wei-zu CHEN, Cun-xin WANG[2]

College of Life Science and Bioengineering, Beijing University of Technology, Beijing 100022, China

KEY WORDS HIV integrase; inhibitors; quinolines; comparative molecular field analysis; AutoDock

ABSTRACT

AIM: To understand pharmacophore properties of styrylquinoline derivatives and to design inhibitors of HIV-1 integrase. **METHODS:** Comparative molecular field analysis (CoMFA) was performed to analyze three-dimensional quantitative structure-activity relationship (3D-QSAR) of styrylquinoline derivatives. Thirty-eight compounds were randomly divided into a training set of 28 compounds and a test set of 10 compounds. The stability of 3D-QSAR models was proved by the analysis of cross-validated and non-cross-validated methods. Moreover, the binding mode of these compounds and integrase was constructed by AutoDock program. **RESULTS:** The CoMFA model of the training compounds was reasonably predicted with cross-validated coefficient (q^2) and conventional (r^2) values (up to 0.696 and 0.754). Then the model was validated by the test set. The resulting CoMFA maps visualized structural requirements for the biological activity of these inhibitors. Docking results showed that a carboxyl group at C-7 and a hydroxyl group at C-8 in the quinoline subunit, bound closely to the divalent metal cofactor (Mg^{2+}) around the integrase catalytic site. Moreover, there is a linear correlation between the binding energy of the inhibitors with integrase and their inhibitory effect. **CONCLUSIONS:** The present study indicated that the CoMFA model together with docking results could give us helpful hints for drug design as well as interpretation of the binding affinity between these inhibitors and integrase.

INTRODUCTION

Along with reverse transcriptase (RT) and protease (PR), HIV integrase (IN) is recognized as an important target for treatment of acquired immunodeficiency syndrome (AIDS). Drugs included in the highly active antiretroviral therapy (HAART)[1] regime are mainly directed against RT and PR. However, toxicities and emergence of drug-resistant virus necessitate the examination of complimentary targets for therapeutic development[2,3]. Accordingly, significant effort is devoted to find inhibitors against the third viral enzyme, IN[4-6].

IN catalyzes the insertion of viral cDNA into the host genome. Integration occurs via a multi-step sequence of reaction, which includes cleavage of a dinucleotide pair from the 3'-end (termed 3'-processing)

[1] Project supported by the National Natural Science Foundation of China (No 30170230), the Beijing Natural Science Foundation (No 5032002 and 5042003), and Beijing City Education Committee (No KZ200410005002).
[2] Correspondence to Prof Cun-xin WANG. Phn 86-10-6739-2724. Fax 86-10-6739-2724. E-mail cxwang@bjut.edu.cn
Received 2003-10-28 Accepted 2004-03-16

followed by transfer of the resulting shortened strands into the target DNA (termed strand transfer). Although a large number of compounds have been reported to inhibit HIV-1 integrase in biochemical assays[6-10], only a few exhibit a substantial level of antiviral activity at nontoxic concentrations and distinct selectivity for IN and no clinically useful inhibitor has been developed to date[7,10]. This requires insights into the factors that influence inhibitor's activity and selectivity toward IN to guide drug design.

The present study has reported styrylquinoline derivatives as potent HIV IN inhibitors. These compounds display antiviral activities in a *de novo* infection assay of CEM cells and are devoid of cytotoxicity[11,12]. Ouali *et al* have analyzed thermodynamic and geometrical parameters of inhibitors binding to the core domain of RSV[13]. Some research groups have developed pharmacophores of different classes of integrase inhibitors including styrylquinoline[14-17]. Despite the remarkable research work, the binding mode of styrylquinoline derivatives to IN and the rational design of new inhibitors remain to be elucidated. Consequently, our primary aim is to obtain the CoMFA[18] model to predict the activity of styrylquinoline derivatives and the rational binding mode of styrylquinoline derivatives to IN. CoMFA and docking simulations were extended to styrylquinoline derivatives in this work. We anticipate this study might give significant information for drug design.

MATERIALS AND METHODS

Data sets To develop reliable CoMFA, 38 styrylquinoline derivatives with diverse structures and distinct activities were selected from two literatures of the same research group[11,12]. The biological activity of each compound expressed as IC_{50}, which is the inhibitory concentration of compounds needed to inhibit 50 % of HIV-1 IN in 3'-processing, was converted to pIC_{50} ($-lgIC_{50}$) for the 3D-QSAR analysis. Thirty-eight derivatives were randomly divided into two groups: a training set of 28 compounds and a test set of 10 compounds.

3D-QSAR studies Three-dimensional structures of these inhibitors were built using SYBYL 6.9[19]. The initial structures were minimized using the semi-empirical program MOPAC 6.0 at the AM1 Hamiltonian[20]. The Mullicken population analysis atomic charges at the AM1 level (AM1-Mul) were considered in the present work. Molecular alignment was carried out using the SYBYL Multifit option. The SYBYL spring constant value was 20 and compound SQ15, one of the most active structures, was used as the alignment template shown in Fig 1.

The CoMFA region was defined to extend 5 Å beyond the van der Waals radii of the assembly of superimposed molecules along each of the principal axes of a Cartesian coordinate system. The grid spacing was set to 2Å in all *x*, *y*, and *z* directions. The default sp^3 carbon atom with a formal charge of +1|e| was selected as the probe atom. In CoMFA calculation, steric (Lennard- Jones 6-12 potential) and electrostatic (Coulombic potential) field were generated with a distance-dependent dielectric at each lattice point and the maximum values were truncated to 30 kcal/mol. Additionally, H-bonding fields were included in the CoMFA study. Once an H-bond CoMFA column has been created, the acceptor and donor components are nominally a "steric" field type component and an "electrostatic" field type component, respectively.

The correlation of the CoMFA descriptor with corresponding pIC_{50} was evaluated by the PLS regression analysis module[21] in SYBYL. To choose the optimum number of principal components and check the statistical significance of the models, cross-validations were performed by means of the Leave-one-out (LOO) procedure in the enhanced version of PLS. The optimum number of components for the training set was determined by the highest cross-validated (q^2) and the smallest predictive error sum of squares (*PRESS*). Finally, the PLS analysis of the predictive 3D-QSAR models was repeated without cross-validation for the optimum component of the training set. Conventional correlation coefficient (r^2) and its standard error (*s*) were computed, and the CoMFA coefficient contour plots were generated. CoMFA columns (ie, values at a given lattice point) were filtered with the cutoff of 2.0 kcal/mol to speed up computation. For the final model to be used to predict the test set, PLS fit was done without filtering.

Molecular docking To further understand the binding mode between styrylquinoline derivatives and HIV-1 IN, these compounds were docked to the core domain of IN by the AutoDock3.0 program[22]. The structure of the IN core domain was taken from the Brookhaven Protein Databank (PDB ID: 1QS4)[23] and the A-chain residues of 1QS4 were remained to dock. The missing residues (141-144) were inserted by using

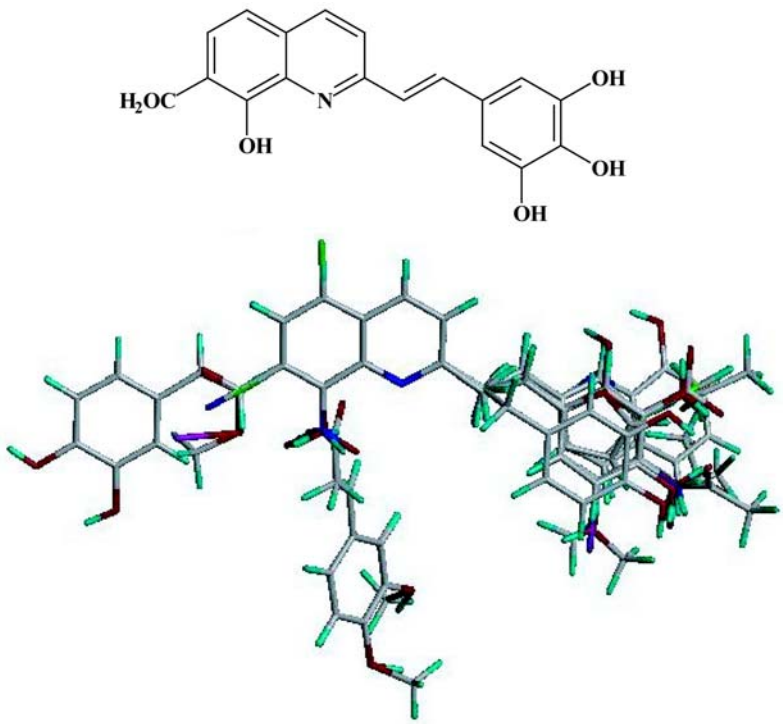

Fig 1. The compound SQ15 used as a template for molecular alignment (the bold face shows the core structure used to perform molecular alignment) and stereoview of all aligned compounds.

the loop search algorithm in SYBYL BIOPOLYMER module. The polar hydrogen atoms and Amber atom charges of A-chain protein were added with SYBYL and the active site magnesium ion was maintained throughout the entire process (with a charge of +2). For ligands, partial atomic charges were added by AM1-Mul charges method with SYBYL.

In docking simulation, the dimensions of the grids were thus 30 Å×30 Å×30 Å with a spacing of 0.375 Å and the center close to OD2 atom of Asp 64. Docking was run using the Lamarckian genetic algorithm and a standard protocol, with a maximum number of energy evaluations of 1.5×10^6 per run, and the other run parameters were maintained at their default settings. There were 20 runs for each system using the optimized run parameters. The results less than 1.0 Å in positional root-mean-square deviation (rmsd) were clustered together and represented by the result with the most favorable free energy of binding.

RESULTS AND DISCUSSION

CoMFA models CoMFA is the versatile and powerful technique for studying the quantitative structure-activity relationship at 3D level (3D-QSAR). It has been successfully applied to guide the design of bioactive molecules[24,25].

Tab 1 lists the PLS results of the CoMFA model using different field combinations. For CoMFA models, the q^2 value changed from 0.597 to 0.621 by adding the

Tab 1. PLS statistic data of CoMFA models[a] obtained from different fields.

	CoMFA 1 Steric+Ele	CoMFA 2 Steric+Ele[c]+ H-bond	CoMFA 3[b] Steric +Ele[c]+ H-bond
q^2	0.597	0.621	0.696
PRESS	0.556	0.528	0.473
r^2	0.765	0.725	0.754
s	0.425	0.450	0.426
F	40.617	68.511	79.657
Components	2	2	1
Fraction			
Steric	0.410	0.186	0.173
Electrostatic	0.590	0.177	0.241
Acceptor		0.344	0.294
Donor		0.294	0.291

[a] Using AM1_Mul Partial Charges and Grid spacing: 1.5 Å. [b] CoMFA model generated after region focus. [c] Ele is the electrostatic field.

H-bonding fields. After region focusing, the q^2 value of the CoMFA model with the steric, electrostatic, and H-bonding fields is distinctly increased (q^2=0.696) because the weights for those meaningful grid points are increased and the noise is decreased. Consequently, the CoMFA 2 model with the steric, electrostatic and H-bonding fields after region focusing was selected as the best CoMFA model. The non-cross-validated PLS analysis yielded the model with r^2 of 0.754 and s of 0.426. Moreover, the best CoMFA model was applied to predict the activities of ten molecules in the test set (r^2_{test}=0.633, s_{test}=0.633). Fig 2 shows the prediction results for the test set with the best CoMFA models.

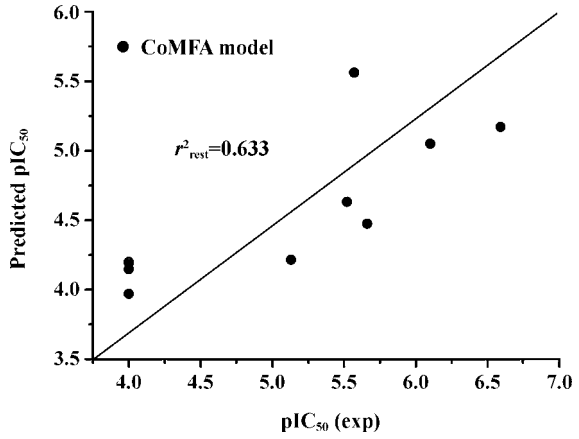

Fig 2. Plots of the predictions of the best CoMFA model for the test-set compounds.

CoMFA contour maps Steric, electrostatic and H-bonding features of the CoMFA model for integration data were shown in Fig 3. These maps showed the changes of molecular fields were associated with differences of biological activity. For reference, SQ15 was displayed inside the field. The model suggested that activity would be favored by the presence of a bulky group near the volume colored green (around the carboxyl group at C-7 in quinoline ring and two hydroxyl groups at C-3' and C-4' in the ancillary phenyl ring), while steric restriction near those colored yellow (around C-8 position). Similarly, positive charge near the blue regions (eg, the region near the H atom in C-7 carboxyl group, N atom of quinoline, and C-3' position of phenyl ring) and negative charge near the red regions (eg, near the carboxyl oxygen atom at C-7) would favor increased activity (Fig 3A). This means that the groups or atoms with positive charge in the blue regions and negative charges in the red regions are very important to ligand

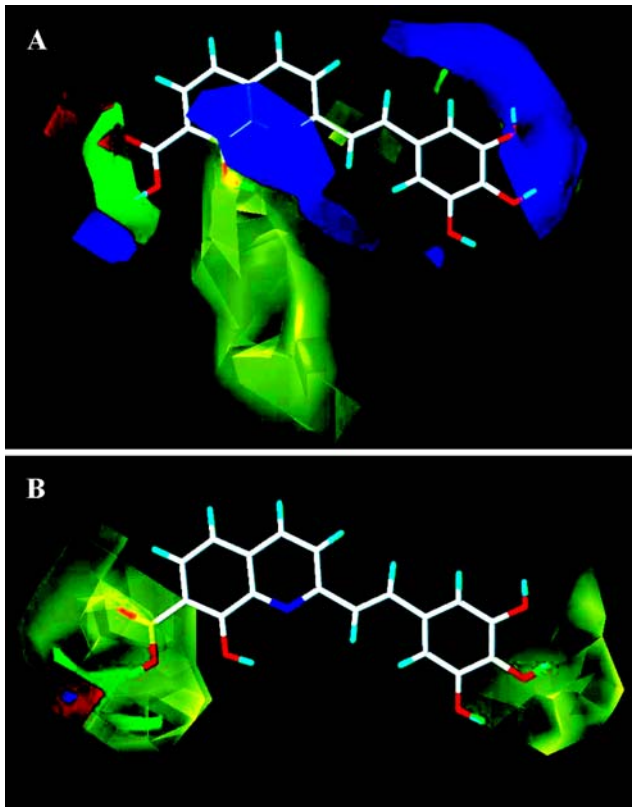

Fig 3. The CoMFA models for styrylquinoline derivatives. A) The contour plot of the CoMFA steric and electrostatic fields. B) The contour plot of the CoMFA H-bonding fields.

binding. For instance, when the C-7 hydrogen atom in compound SQ27 is substituted with carboxylic group to give compound SQ2, inhibitory potency will be improved more than 20-fold. The compounds of SQ24 and SQ25 with a bulky group at C-8 position exhibit a poor antiviral activity (pIC_{50}=4.00).

The H-bonding field contributions were shown in Fig 3B. From the fraction of field, the H-bonding acceptor field was slightly more important than the other fields. The contour indicated that more H-bonding acceptor groups in the green region increased potency, whereas more H-bonding acceptor groups in the yellow regions (near hydroxyl groups at C-3', C-4', C-5' and C-8) decreased potency. The H-binding donor favorable areas were marked blue color, while the H-binding donor unfavorable areas were labeled red. The blue region was near the OH of C-7 carboxyl group, namely, the OH might form the stable H-bond with some residues in protein. For example, the methylation of the carboxylic group in compound SQ12 to give compound SQ20 can make inhibitory potency drop 50-fold.

The CoMFA results described similarities and differences between these compounds and correlated them

with changes in the antiviral activity. The results reflected structural requirements for biological activity from the inhibitors, hence we further explore the binding mode between styrylquinolines and IN.

Binding mode prediction of styrylquinolines / IN Most of the compounds possess various sites of possible protonation. For instance, SQ12 has protonation sites at N and at the oxygen atoms of C-7, C-8, C-3', and C-4'. As the two p*K*a values of catechol in aqueous solutions are 9.45 and 12.8 (the second one is questionable)[26], catechol is not ionized in the reaction buffer, and the chemical formula of the catechol moiety of the drugs is shown in Tab 2. In contrast, *o*-hydroxybenzoic acid has two p*K*a values 2.98 (CO_2H/CO_2^-) and 12.38 (OH/O^-)[27]. According to the spectroscopic studies of Bardez *et al*[28] on 8-hydroxyquinoline, the proton belongs to the hydroxyl group in the ground state but migrates to N in the excited state. The ground-state p*K*a of 8-hydroxyquinoline in aqueous solutions at 20 ºC are 5.13 (NH+/N) and 9.89 (OH/O-)[29]. As a consequence, compounds from SQ1 to SQ20 probably have a net charge of -1, SQ38 compound has a charge of -2, and the other has a zero charge. In our work, the binding mode of styrylquinoline compounds with various protonation and integrase were analyzed by AutoDock program.

As labeled in Fig 4A, the well-clustered docking results were obtained for most of investigated ligands (SQ1-SQ22, SQ30-SQ38). The docking of these compounds produced the two clusters occupying two separate but overlapping binding regions. The two clusters occupy a narrow binding region formed by Asp64, Ser66, His67, Leu68, Gly70, Asp116, Gln148, Gly149, Glu152, Asn155, Lys156, and Lys159. In the present work, the styrylquinoline inhibitors were different from the cinnamoyl inhibitors studied by Buolamwini *et al*[30]. The styrylquinoline compounds lie in a nearby coordination to magnesium cation. As shown in Fig 4B, compound SQ15 as a template was displayed in the binding site. The oxygen atoms of C-7 carboxyl group and C-8 hydroxyl group may coordinate with Mg^{2+} ion within the enzyme catalytic site. This docking mode was the same as the experiment report given by Zouhiri *et al*[12]. Additionally, the estimated docking energies, ranks and

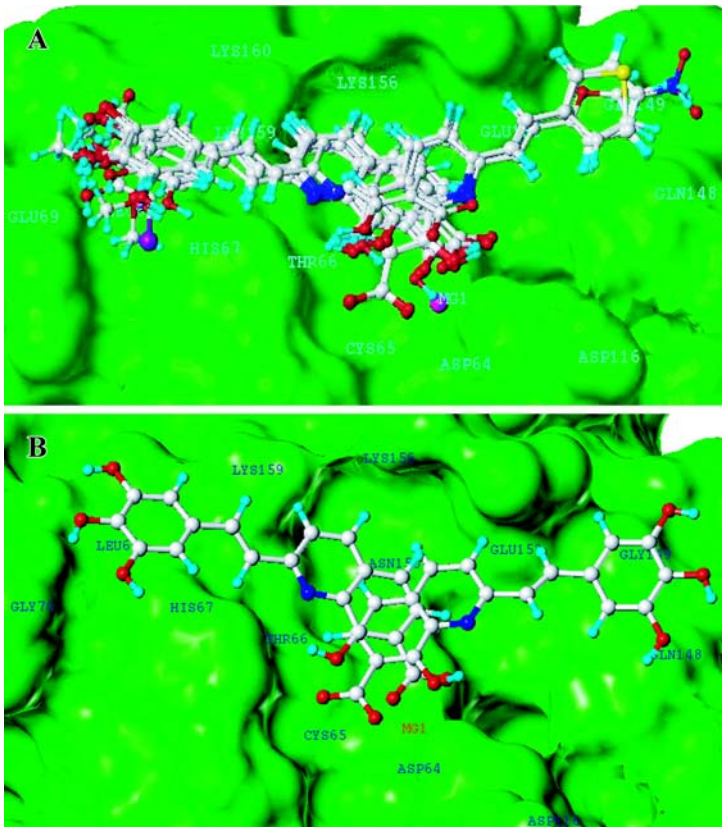

Fig 4. The binding mode of styrylquinoline derivatives to IN. A) The docking cluster of styrylquinoline compounds in the IN active site. B) Superimposition of one docked structure (SQ15) over physicochemical properties of the IN active site.

Tab 2. Structures, HIV-1 IN inhibitory activity, and docking results of styrylquinoline derivatives.

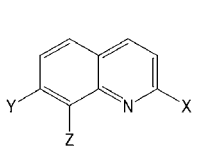

SQ1-SQ20, SQ22-SQ38

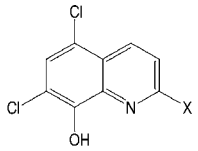

SQ21

Comp	X	Y	Z	pIC_{50}	ΔG_b	Rank	N
SQ1	Me	CO_2H	OH	4.00	-8.29	1	8
SQ2	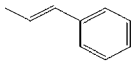	CO_2H	OH	5.28	-9.40	1	6
SQ3	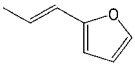	CO_2H	OH	5.72	-9.43	1	8
SQ4	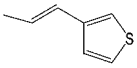	CO_2H	OH	5.47	-9.78	1	14
SQ5	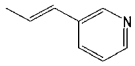	CO_2H	OH	5.39	-9.13	1	13
SQ6	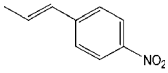	CO_2H	OH	5.92	-9.17	1	14
SQ7	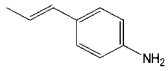	CO_2H	OH	5.46	-9.37	1	15
SQ8	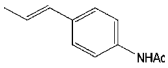	CO_2H	OH	5.85	-9.46	1	14
SQ9	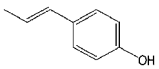	CO_2H	OH	5.80	-9.32	1	15
SQ10	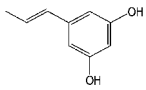	CO_2H	OH	5.49	-9.31	1	11
SQ11	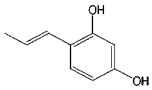	CO_2H	OH	5.43	-9.28	1	7
SQ12	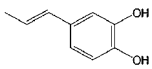	CO_2H	OH	5.62	-9.26	1	4
SQ13	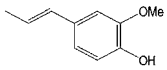	CO_2H	OH	5.55	-9.19	1	6
SQ14	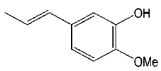	CO_2H	OH	6.05	-9.70	1	10
SQ15	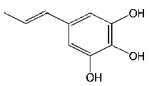	CO_2H	OH	6.52	-9.14	1	15
SQ16	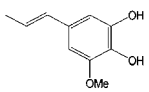	CO_2H	OH	6.15	-9.42	1	4
SQ17	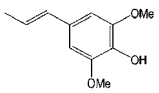	CO_2H	OH	5.31	-9.26	1	7
SQ18	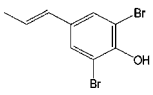	CO_2H	OH	5.89	-9.84	1	16

(Continue)

Comp	X	Y	Z	pIC_{50}	ΔG_b	Rank	N
SQ19	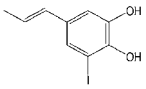	CO_2H	OH	5.40	-9.38	1	13
SQ20	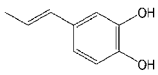	CO_2Me	OH	4.00	-7.68	1	6
SQ21	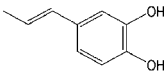			4.00	-7.15	1	7
SQ22	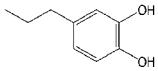	CO_2H	OH	5.64	-9.33	1	5
SQ23	Me	H	OH	4.00	-6.03	1	8
SQ24	Me	H	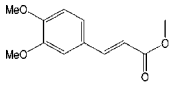	4.00	-8.02	1	18
SQ25	Me	H	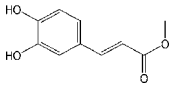	4.00	-8.59	1	12
SQ26	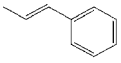	H	OAc	4.00	-8.16	1	14
SQ27	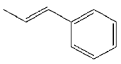	H	OH	4.00	-7.76	1	17
SQ28	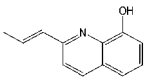	H	OH	4.00	-7.53	1	19
SQ29	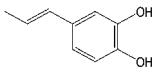	H	H	4.00	-7.73	1	15
SQ30	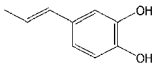	H	NO_2	4.00	-7.91	1	14
SQ31	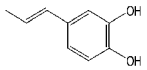	H	NH_2	4.00	-8.48	1	16
SQ32	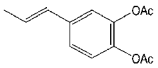	H	OAc	4.00	-8.45	1	12
SQ33	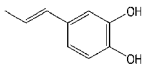	H	OH	5.13	-8.63	1	11
SQ34	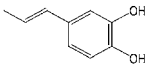	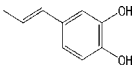	OH	5.66	-8.93	1	3
SQ35	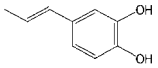	CN	OH	5.52	-8.67	1	3
SQ36	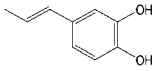	CO_2Na	OH	6.10	-9.30	1	11
SQ37	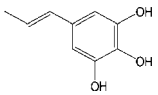	CO_2Na	OH	6.58	-9.17	1	9
SQ38	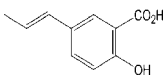	CO_2H	OH	5.57	-9.74	1	10

ΔG_b is the estimated binding free energy of the cluster results for the best binding site and is given in kcal/mol; Rank is the scoring of the cluster in 20 docked structures; N is the number of the structures involved in the cluster.

the number of the structures involved in the clusters were calculated by AutoDock and listed in Tab 2. The estimated docking energy correlated well with the biological activity pIC_{50} in a general sense, and compounds with the higher activity showed the lower AutoDock energy scores (Tab 2). This correlation was more pronounced for molecules that differed mostly by the presence of a carboxyl group at C-7 and a hydroxyl group at C-8, and their absence or methylation. Consequently, we have proposed the two orientations to be probably the best binding mode for the styrylquinoline inhibitors at the IN active site. The docking results together with the 3D-QSAR contour plots clearly demonstrate that the presence of a carboxyl group at C-7, a hydroxyl at C-8 and an aromatic ring is required for the biological activity and the binding mode of these compounds. Additionally, we suggest that adding H-bonding acceptors at C-3 in the quinoline ring would form H-bonds with the surface residues in IN to improve biological activities of styrylquinoline inhibitors.

CONCLUSION

In this study, the CoMFA models show reasonably predictability to estimate the biological activity of the styrylquinoline compounds. The CoMFA contour maps also visualize structural similarities and differences among the styrylquinoline compounds and show that the functional group and region will affect the antiviral activity of the inhibitors in three-dimensional space. On the other hand, molecular docking simulation shows one potential binding mode of these compounds to IN. As shown in docking results, a carboxyl group at C-7 and a hydroxyl group at C-8 in the quinoline subunit interact with the divalent metal cofactor within the IN catalytic site. The binding mode is highly complementary to the analysis from the experiment. Results from the present study demonstrate the utility of CoMFA 3D-QSAR models and molecular docking as predictors of inhibitor-IN binding affinity. Computer screening base on the results is in progress. In addition, in order to get a more native-like binding mode of these inhibitors with IN, the minimization of docking structures and the CoMFA study with the optimized docking alignment is currently underway.

ACKNOWLEDGMENT We thank Prof OLSON for providing us the AutoDock program. We also thank Dr Ting-jun HOU and Yi-hua WANG for helpful suggestions.

REFERENCES

1 Caliendo AM, Hirsch TN, Liu B, Pattabiraman N, Erickson JW. Combination therapy for infection due to human immunodeficiency virus type 1. Clin Infect Dis 1994; 18: 516-24.
2 Appelt K, Clare M, Pettit S, Michael SF, Swantsrom R, Moore MC, *et al*. Therapeutic approaches to HIV. Perspect Drug Discov Des 1993; 1: 123-8.
3 Condra JH, Schleif WA, Blahy OM, Gabryelski LJ, Graham DJ, Quintero JC, *et al*. *In vivo* emergence of HIV-1 variants resistant to multiple protease inhibitors. Nature 1995; 374: 569-71.
4 Pommier Y, Neamati N. Inhibitors of human immunodeficiency virus integrase. Adv Virus Res 1999; 52: 427-58.
5 Pluymers W, De Clercq E, Debyser Z. HIV-1 integration as a target for antiretroviral therapy: a review. Curr Drug Targets Infect Disord 2001; 1: 133-49.
6 Pommier Y, Marchand C, Neamati N. Review retroviral integrase inhibitor year 2000: update and perspectives. Antiviral Res 2000; 47: 139-48.
7 Hazuda DJ, Felock P, Witmer M, Wolfe A, Stillmock K, Grobler JA, *et al*. Inhibitors of strand transfer that prevent integration and inhibit HIV-1 replication in cells. Science 2000; 287: 646-50.
8 Young SD. Inhibition of HIV-1 integrase by small molecules: the potential for a new class of AIDS chemotherapeutics. Curr Opin Drug Discov Devel 2001; 4: 402-10.
9 Jing N, Hogan ME. Structure-activity of tetrad-forming oligonucleotides as potent anti-HIV therapeutic drug. J Biol Chem 1998; 273: 34992-9.
10 Craigie R. HIV integrase, a brief overview from chemistry to therapeutics. J Biol Chem 2001; 276: 23213-6.
11 Mekouar K, Mouscadet JF, Desmaële D, Subra F, Leh H, Savoure D, *et al*. Styrylquinoline derivatives: a new class of potent HIV-1 integrase inhibitors that block HIV-1 replication in CEM cells. J Med Chem 1998; 41: 2846-57.
12 Zouhiri F, Mouscadet JF, Mekouar K, Desmaële D, Savouré D, Leh H, *et al*. Structure-activity relationships and binding mode of styrylquinolines as potent inhibitors of HIV-1 integrase and replication of HIV-1 in cell culture. J Med Chem 2000; 43:1533-40.
13 Ouali M, Laboulais C, Leh H, Gill D, Desmaële D, Mekouar K, *et al*. Modeling of the inhibition of retroviral integrases by styrylquinoline derivatives. J Med Chem 2000; 43: 1949-57.
14 Makhija MT, Kulkarni VM. Design value analysis of HIV-1 integrase inhibitors. J Chem Inf Comput Sci 2001; 41: 1569-77.
15 Yuan H, Parrill AL. QSAR studies of HIV-1 integrase inhibition. Bioorg Med Chem 2002; 10: 4169-83.
16 Makhija MT, Kulkarni VM. QSAR of HIV-1 integrase inhibitors by genetic function approximation method. Bioorg Med Chem 2002; 10: 1483-97.
17 Makhija MT, Kulkarnl VM. Molecular electrostatic potentials as input for the aligment of HIV-1 integrase inhibitors in 3D QSAR. J Comput Aided Mol Des 2001; 15: 961-78.

18 Cramer RD, Patterson III DE, Bunce JD. Comparative molecular field analysis (CoMFA) 1 effect of shape on binding of steroids to carrier proteins. J Am Chem Soc 1988; 110: 5959-67.
19 Sybyl [molecular modeling package], version 6.9, St Louis (MO): Tripos Associates; 2000.
20 Dewar MJS, Zoebisch EG, Healy EF, Stewart JJP. Development and use of quantum mechanical molecular models. 76. AM1: a new general purpose quantum mechanical molecular model. J Am Chem Soc 1985; 107: 3902-9.
21 Bush BL, Nachbar RB Jr. Sample-distance partial least squares: PLS optimized for many variables, with application to CoMFA. J Comput Aided Mol Des 1993; 7: 587-619.
22 Morris GM, Goodsell DS, Halliday RS, Huey R, Hart WE, Belew RK, *et al*. Automated docking using a lamarckian genetic algorithm and an empirical binding free energy function. J Comput Chem 1998; 19: 1639-62.
23 Goldgur Y, Craigie R, Cohen GH, Fujiwara T, Yoshinaga T, Fujishita T, *et al*. Structure of the HIV-1 integrase catalytic domain complexed with an inhibitor: a platform for antiviral drug design. Proc Natl Acad Sci USA 1999; 96: 13040-3.
24 Bohm M, Stuzerbercher J, Kliebe G. Three-dimensional quantitative structure-activity relationship analysis using comparative molecular field analysis and comparative molecular similarity indices analysis to elucidate selectivity differences of inhibitors binding to trypsin, thrombin, and factor xa. J Med Chem 1999; 42:458-77.
25 Debnath AK. Comparative molecular field analysis (CoMFA) of a series of symmetrical *bis*-benzamide cyclic urea derivatives as HIV-1 protease inhibitors. J Chem Inf Comput Sci 1998; 38: 761-7.
26 Timberlake C. Potentiometric and polargraphic study of copper catechol complexes. J Chem Sco 1957; 997: 4987-93.
27 Branch GEK, Yabroff DL. The anomalous strength of salicylic acid. J Am Chem Soc 1934; 56: 2568-70.
28 Bardez E, Devol I, Larrey B, Valeur B. Excited-state processes in 8-hydroxyquinoline: photoinduced tautomerization and solvation effects. J Phys Chem B 1997; 101: 7786-93.
29 Albert A, Phillips JN. Ionization constants of heterocyclic substances. Part II: Hydroxy derivatives of nitrogenous sixmembered ring compounds. J Chem Soc 1956; 264: 1294-304.
30 Buolamwini JK, Assefa H. CoMFA and CoMSIA 3D QSAR and docking studies on conformationally-restrained cinnamoyl HIV-1 integrase inhibitors: exploration of a binding mode at the active site. J Med Chem 2002; 45: 841-52.